Quasi-liquid layers in grooves of grain boundaries and on grain surfaces of polycrystalline ice thin films

Jialu Chen[1], Takao Maki[2], Ken Nagashima[1], Ken-ichiro Murata[1], Gen Sazaki[1,]*

1 Institute of Low Temperature Science, Hokkaido University, N19-W8, Kita-ku, Sapporo 060-0819, Japan

2 Optical Design Maki, 4-58-603 Inadaira, Murayama, Tokyo 208-0023, Japan

* To whom correspondence should be addressed. E-mail: sazaki@lowtem.hokudai.ac.jp

KEYWORDS: surface melting, quasi-liquid layers, polycrystalline ice thin film, grain boundary, grain surface

ABSTRACT

In nature, a large proportion of ice is present in a polycrystalline state. Thus, understanding the formation of quasi-liquid layers (QLLs) on/in polycrystalline ice is indispensable for understanding a wide variety of natural phenomena. In this study, we observed surfaces of polycrystalline ice thin films using our advanced optical microscope. We focused our attention on the macroscopic fluidity of objects observed on polycrystalline ice surfaces as evidence for the presence of QLLs. Systematic observations under various temperatures and water vapor pressures showed that, with increasing temperature, QLLs first appeared preferentially in grooves of grain boundaries and continued to exist at −1.9±0.4 °C, irrespective of the water vapor pressure (even in immediate vicinities of the vapor–ice equilibrium curve). From this result, we concluded that the QLLs were formed by melting of grain boundaries to relax lattice mismatches. With a further increase of temperature, droplet-type QLLs appeared on grain surfaces at −0.7±0.2 °C. However, as time elapsed, the droplet-type QLLs on the grain surfaces spontaneously disappeared within 5±3 min even though temperature and water vapor pressure were kept constant. Such appearance and subsequent disappearance of the droplet-type QLLs on the grain surfaces were observed even under relatively-highly supersaturated and undersaturated conditions.

1. INTRODUCTION

A vast amount of ice exists on the earth, and surface melting of ice forms thin liquid water layers, so-called quasi-liquid layers (QLLs), on ice surfaces even below the melting point of ice (0°C).[1-3] Because QLLs govern properties of ice surfaces just below the melting point, surface melting of ice plays critically important roles in a wide range of phenomena, including the preparation of a snow ball,[4] frost heave,[1, 5] slipperiness of ice,[1, 2] regelation,[1, 6] conservation of tissues and foods,[7, 8] and electrification of thunderclouds.[1] Therefore, unraveling the surface melting of ice is indispensable for understanding these phenomena.

In nature, a large proportion of ice is present in a polycrystalline state. Hence, understanding the behavior of QLLs in grain boundaries and on grain surfaces of polycrystalline ice is important. Although numerous researchers have studied the formation of QLLs on single ice crystals (see reviews[1-3, 9, 10] and references therein), experimental studies on the formation of QLLs on/in polycrystalline ice have been limited. Marder observed the geometries of veins and nodes in polycrystalline ice,[11] and studied the effects of impurities on the vein width.[12] In addition, two groups have studied the behavior of grain boundaries experimentally. Lu et al. investigated the diffusion of D_2O in polycrystalline H_2O ice by thermal desorption spectroscopy and concluded that grain-boundary premelting is implausible at temperatures as high as –2 °C.[13] Thomson et al. optically measured thin water layers in grain boundaries using bicrystals, and investigated the effects of impurities on the thickness of the water layers.[14, 15] They found that the thickness of grain boundaries increased in the range 1–10 nm with increasing impurity concentration at ~1.5 K undercooling. The relatively small thickness (<10 nm) of grain boundaries indirectly supported the results of Lu et al.[13] However, agreement with theoretical predictions was not attained.[15] Furthermore, the abrupt grain-boundary melting predicted theoretically[16, 17] has not yet been observed experimentally. Therefore, to obtain a

unified understanding, further experimental studies on the behavior of QLLs on/in polycrystalline ice are highly required.

Recently, we observed surfaces of polycrystalline ice thin films using a Michelson interferometer (2.5× magnification) attached to a laser confocal microscope (LCM).[18] From the optical isotropy observed under a crossed-nicols condition, we determined that QLLs appeared on the polycrystalline ice surfaces.[18] However, after this paper was published,[18] we combined a Linnik interferometer (20× magnification) with the LCM and found that we lost the experimental evidence from which we deduced the presence of QLLs in the previous paper;[18] for details, see our correction.[19] Therefore, further studies based on more reliable evidence are necessary to reveal the behavior of QLLs on polycrystalline ice surfaces.

In the present study, we directly observed the macroscopic fluidity of QLLs using an LCM combined with a differential interference contrast microscope[20, 21] (LCM-DIM) and used this fluidity as much more direct and reliable evidence for the presence of QLLs. We systematically observed surfaces of polycrystalline ice thin films under various pressure–temperature conditions. We found two temperature ranges in which QLLs, showing macroscopic fluidity, were formed in grooves of grain boundaries (–1.9 ± 0.4 °C) and on grain surfaces (–0.7 ± 0.2 °C). We first describe typical polycrystalline ice grains and their grain growth behavior (section 3.1), and then show the appearance of QLLs in grooves of grain boundaries (section 3.2) and on grain surfaces (section 3.3). We also discuss the stability of QLLs on polycrystalline ice surfaces.

2. EXPERIMENTAL PROCEDURES

2.1. Preparation of Polycrystalline Ice Thin Film. A round cover glass (12 mm in diameter) was placed on an aluminum block cooled at −196 °C with liquid N_2. Approximately 5 μL of

ultra-pure water (resistivity: 18 MΩ·cm) was dropped onto the cover glass from 1.2 m above. A polycrystalline ice thin film 7–9 mm in diameter and 70–80 μm in thickness formed on the cover glass. The polycrystalline ice thin film was cut into a small piece (approximately 0.6 × 0.6 mm^2), and the remaining part of the film was removed from the cover glass to reduce the amount of water vapor necessary for the growth of the ice thin film and to reduce the depletion of water vapor in the vicinity of the growing ice thin film, as described in our previous paper.[22] The ice thin film on the cover glass was placed in an observation chamber. After the pure water was dropped onto the cover glass, all processes were carried out in a cold room at −10 °C. For details, see our previous report.[18]

2.2. Observation System. Our custom-made observation chamber is schematized in Fig. 1. The observation chamber was made of two Cu plates. The temperatures of the upper and lower Cu plates, T and T_{source}, were separately controlled using Peltier elements. The polycrystalline ice thin film formed on the cover glass was placed at the center of the upper Cu plate. On the lower Cu plate, ice crystals were also grown to supply water vapor to the polycrystalline ice thin film for the observation. The total pressure in the observation chamber was kept at atmospheric pressure by filling the chamber with pure nitrogen gas (see the section 2.3). The volume of the ice crystals for supplying water vapor was substantially larger than that of the polycrystalline ice thin film. Hence, the partial pressure of water vapor P in the observation chamber was determined by T_{source}. In addition, the equilibrium partial vapor pressure P_e for the polycrystalline ice thin film was determined by T. The supersaturation of the water vapor, $\sigma = P/P_e$, was adjusted by changing T_{source} and T. The parameters P and P_e had errors of ±2 Pa. Hence, σ had an error of ±0.004. Details of the chamber and its operation are explained elsewhere.[21, 22]

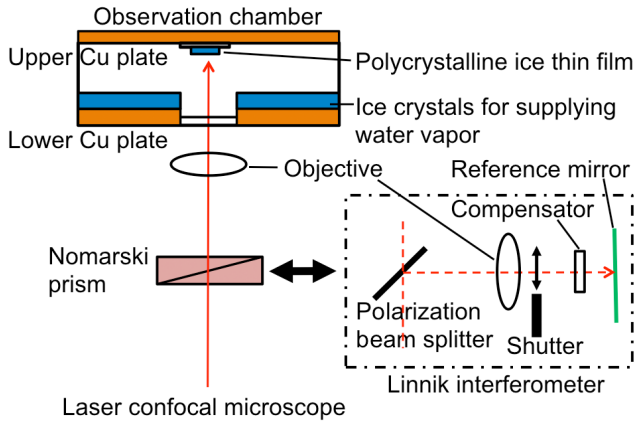

Fig. 1

As shown in Fig. 1, through a glass window at the center of the lower Cu plate, the polycrystalline ice thin film was observed using a laser confocal microscope combined with a differential interference contrast microscope (LCM-DIM):[20, 21] a laser confocal system (Olympus Corp., model FV300) was combined with an inverted optical microscope (Olympus Corp., model IX70). An objective with 20× magnification (Olympus Corp., model LMPlanFL N 20×) was used with the LCM-DIM. A super luminescent diode (Amonics Ltd., model ASLD68-050-B-FA), whose wavelength and coherent length were 680 nm and 10 μm, respectively, was used as a light source. The LCM-DIM can provide three-dimensional contrast to subnanometer-height steps on flat crystal surfaces.[21] In addition, a Nomarski prism could be easily replaced with a Linnik interferometer (Optical Design Maki: 20× magnification) (Fig. 1). The Linnik interferometer was used to monitor the growth and sublimation of polycrystalline ice surfaces.

2.3. Injection of Pure N_2 Gas. After the observation chamber was placed on the observation system, the temperature of the polycrystalline ice thin film and the water vapor pressure in the chamber were set at $T = -9.0$ °C and $P = 288$ Pa ($P_e = 284$ Pa), respectively. Pure N_2 gas was then injected into the observation chamber at a flow rate of 0.4 L/min for 10 min. During the injection of the N_2 gas, the top 3–4 μm of the polycrystalline ice surface was sublimated (monitored using the Linnik interferometer combined with the LCM) to obtain a fresh

(uncontaminated) surface. With the injection of the N_2 gas, the air in the observation chamber (inner volume: ~5 mL) was fully replaced with pure N_2 gas at atmospheric pressure to avoid possible bias caused by atmospheric reactive gasses. After the injection of the N_2 gas, the observation chamber was kept airtight and then used for further observation.

3. RESULTS AND DISCUSSION

3.1. Polycrystalline Ice Thin Films and Their Grain Growth Behavior. Figure 2 shows a polycrystalline ice thin film at T = −2.1 °C and P = 534 Pa (P_e = 514 Pa). Figures 2B1–2B4 show the time course of the LCM-DIM images of the area marked by the dotted rectangle in Fig. 2A. As indicated by black arrows, some grains exhibited relatively fast grain growth on a time scale of approximately 30 min. A comparison between Figs. 2A and 2C shows that some other grains (marked by black arrowheads in Fig. 2C) exhibited relatively slow grain growth. Such substantial variation in the speed of grain growth is likely due to variation in the characteristics of the grain boundaries. The relation between the characteristics of grain boundaries and the misorientation of grains has long been well understood in metallurgy,[23-25] and pioneering works on grain boundaries in ice crystals have also been reported.[26-28]

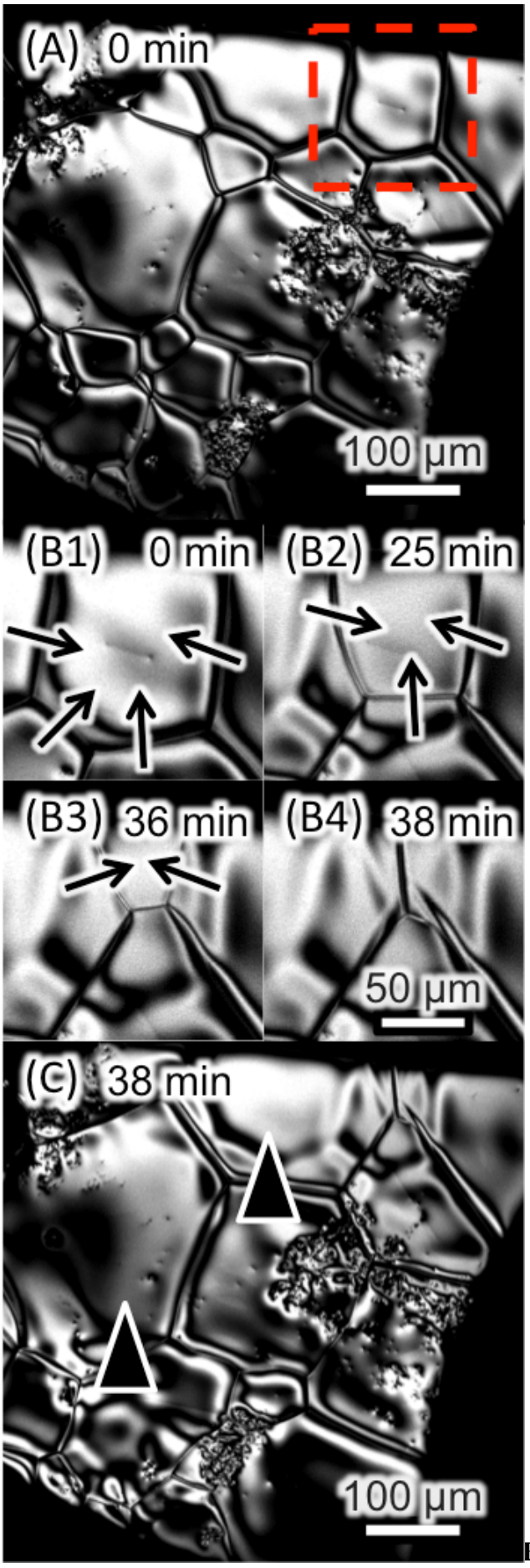
(A) 0 min
100 μm
(B1) 0 min
(B2) 25 min
(B3) 36 min
(B4) 38 min
50 μm
(C) 38 min
100 μm

Fig. 2

We performed similar observations at various *T*s and *P*s. The average lateral size of grains was 170 ± 75 μm. To eliminate the effects of grain growth, we excluded grains that exhibited relatively fast grain growth (within ~30 min) from further examinations of the appearance of QLLs.

3.2. QLLs in Grooves of Grain Boundaries. To reveal the behavior of QLLs on the polycrystalline ice thin films, we further observed the thin film by LCM-DIM. Figure 3 shows the pressure–temperature (*P*–*T*) regions (shown in blue and red colors in the supersaturated and undersaturated conditions, respectively) in which QLLs exist kinetically (and also continuously) on the surfaces of ice single crystals.[29, 30] In the vicinity of the vapor–ice and vapor–liquid water equilibrium curves (solid and dotted curves), QLLs cannot exist kinetically on ice single crystals. In this study, we observed polycrystalline ice thin films systematically under various *P*–*T* conditions and found two temperature ranges in which specific events occurred in grooves of grain boundaries (–2.6 to –1.1 °C) and on grain surfaces (–1.2 to –0.4 °C). Black and red arrows show temperature changes (at constant pressures) that we induced; the results are explained later in the discussion of Figs. 4 and 7, respectively.

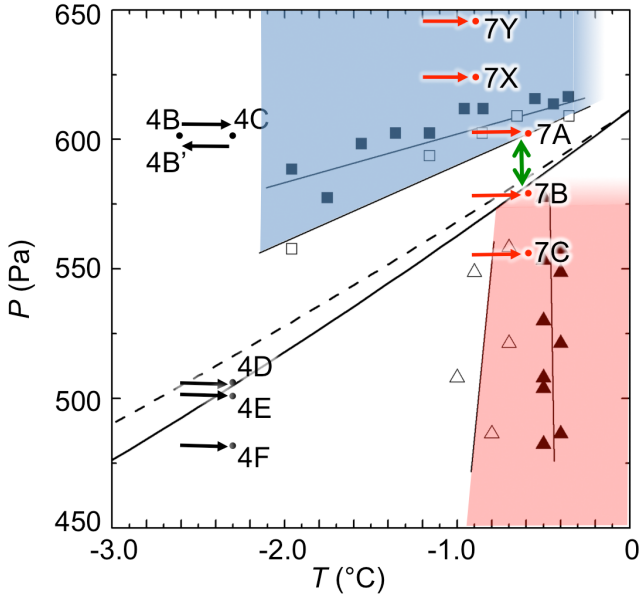

Fig. 3

Figure 4 shows LCM-DIM images of a surface of a polycrystalline ice thin film. To monitor the appearance of QLLs in grooves of grain boundaries, we added polystyrene particles to pure water (653 nm in diameter and 0.02% in volume fraction) when we prepared the polycrystalline ice thin films. In Fig. 4A, white arrowheads indicate polystyrene particles located in a groove of a grain boundary and on a grain surface; we observed a mixture of differential interference contrast and part of the light scattered from the particles (for the former, see the first paragraph in section 3.3). Figure 4B shows the time course of LCM-DIM images in the area marked by the dotted rectangle in Fig. 4A at –2.6 °C.

In the following, the *P*–*T* conditions correspond to points 4B–4F in Fig. 3. In Fig. 4B, we observed no movement of the particle in the groove. By contrast, when the temperature was increased to –2.3 °C (at constant *P*), the particle moved in one direction along the groove, as shown in Fig. 4C and Video S1 in the supporting information. After we recorded the images in Fig. 4C, we lowered the temperature to –2.6 °C again (at constant *P*) and recorded additional images. Figure 4B′ indicates that the particle position was fixed, as observed in Fig. 4B. The temperature change from –2.6 to –2.3 °C (and also that from –2.3 to –2.6 °C) was completed within 1 min. In these images, a time of 0 s corresponds to the moment when the temperature became constant after the temperature change. We repeated similar observations while changing the temperature and found that the starting and stopping temperatures for particle movement in the same groove were highly reproducible.

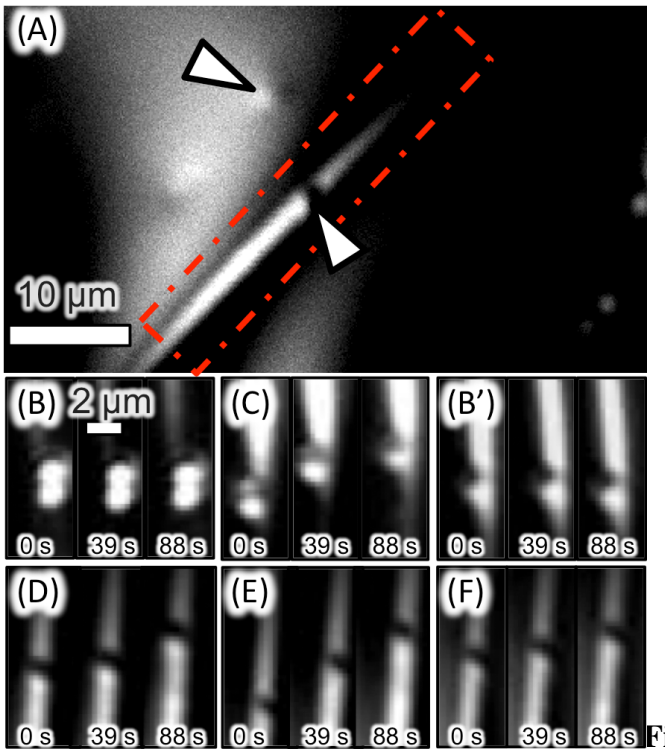

Fig. 4

We performed similar observations by increasing the temperature from –2.6 to –2.3 °C under different water vapor pressures, as indicated by points 4D, 4E, and 4F in Fig. 3. Figures 4D–4F clearly demonstrate that, irrespective of the water vapor pressure, the particle moved along the grooves at –2.3 °C. In addition, the particles continued to move for more than 5 h when *P* and *T* were constant. Notably, the particle located on the grain surface (Fig. 4A) never changed its position during the observation in Fig. 4 because of the absence of QLLs on the grain surface (data not shown).

What do the movements of the particles mean? In this temperature range, grain growth and thermal roughening occurred. Hence, the deformation of grains during such processes could also change the positions of the polystyrene particles in the grooves. However, as shown in Fig. 2, even the relatively fast grain growth at –2.1 °C proceeded on the time scale of 30 min. In this temperature range, thermal roughening occurred over 15 min to 7 h.[31] By contrast, we could observe substantial movements of the particles within 100 s (Figs. 4C–4F). Hence, on the basis of the dramatic difference in time scales, we concluded that the movements of the particles

indicated the appearance of a volume of liquid water sufficient to move them. That is, the immobile particles in the grooves (Figs. 4B and 4B′) demonstrated that no liquid water existed in the grooves of the grain boundaries or that the volume of liquid water was insufficient to move the particles. Here, we note that the absence of movement of the particles at –2.6 °C was not due to an increase in the viscosity of the liquid water because the viscosity of supercooled water at 0 and –2.6 °C is 1.8 and 2.0 (mPa·s),[32] respectively; thus, the increase in viscosity was moderate.

Can the liquid water that appeared in the grooves be considered a QLL? The movement of the 653-nm-diameter polystyrene particles shows that the thickness of the liquid water in the grooves was comparable to the size of the particles. However, in our previous studies, the thickness of droplet-type QLLs that appeared on basal faces ranged from several tens of nanometers to 1 μm.[30, 33] Nevertheless, the droplet-type QLLs exhibited a viscosity 20 times higher than that of bulk water.[34] Hence, the thickness of the liquid water in the grooves was also comparable with that of the QLLs on basal faces. In addition, if "real bulk water" exists on ice crystal surfaces, the bulk water can exist only for very short time period because the normal growth of ice crystals in a bulk melt is extremely fast (10^{-2} to 10^{-7} m/s).[35-38] Hence, we concluded that the liquid water that appeared in the grooves was a QLL.

In Figs. 4C–4F, the particles did not exhibit random (Brownian) motion but rather unidirectional motion. On basal and prism faces of ice single crystals, such unidirectional motion of droplet-type and thin-layer-type QLLs is often observed[33] (readers can view the unidirectional motion of droplet-type and thin-layer-type QLLs on grain surfaces in Videos S3 and S4). The unidirectional motion is likely due to nonuniformity in temperature and water vapor pressure,[39] although the actual reason is still unclear.

As shown in Fig. 4, at –2.3 °C, QLLs, whose volumes were sufficient to move the particles, appeared in the grooves of grain boundaries, irrespective of the water vapor pressure, i.e., even in the immediate vicinity of the vapor–ice equilibrium curve (points 4D and 4E in Fig. 3). This result clearly indicates that the QLLs in the grooves were supplied by the grain boundaries. Figure 5 shows the relation between the free energy of ice crystals (Ice), the grain boundaries (G.B.), QLLs in the grain boundaries (QLLs in G.B.), and QLLs in the groove of grain boundaries (QLLs in G.G.). In general, grain boundaries are substantially more unstable than a crystal because lattice mismatches, which are caused by the contacts of adjacent ice grains with different crystallographic orientations,[23-25] generate strain energy. In Fig. 5, because a grain boundary (a two-dimensional object) is not a phase, a dry grain boundary (Dry G.B. in Figs. 5A-1 and 5B-1) here indicates a grain boundary and adjacent ice thin layers (slabs) in which the strain energy of the grain boundary is distributed. After a dry grain boundary is melted with increasing temperature, QLLs that form in the grain boundary (QLLs in G.B. in Figs. 5A-2 and 5B-2) substantially relax the lattice mismatches. Hence, the QLLs in the grain boundary are as stable as the ice crystal. In such a case, the QLLs formed in the grooves of the grain boundary (QLLs in G.G.) can be reasonably assumed to also be as stable as the QLLs in the grain boundaries because the QLLs in the grain boundary and the QLLs in the groove are formed even in the equilibrium condition. Hence, after the dry grain boundary is melted, the QLLs in the grain boundary and the QLLs in the groove become thermodynamically stable. Although the QLLs in the grain boundary supply the QLLs in the groove, we distinguished these QLLs because two phases (the QLLs and the ice crystal) coexist in the QLLs in the grain boundary, whereas three phases (the QLLs, the ice crystal, and the water vapor) coexist in the QLLs in the groove.

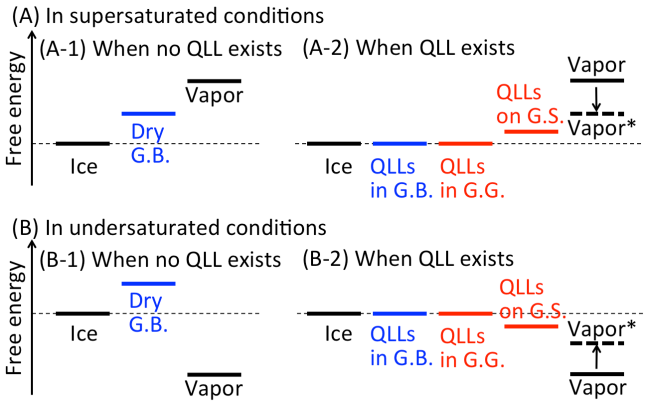

Fig. 5

We speculated that such grain-boundary melting occurred continuously with increasing temperature; i.e., if we use particles with a smaller diameter, we should detect the movement of particles at a temperature lower than –2.3 °C, although we have no experimental evidence to support this claim. In the present study, the amount of QLLs in the grooves of the grain boundaries was not large for the water level of the QLLs in the grooves to be determined using the LCM-DIM and the Linnik interferometer. Spillover of the QLLs from the grooves of the grain boundaries did not occur.

We similarly observed different grain boundaries in different samples and found that, in rare cases, we could not observe unidirectional motion of the particles but could observe their Brownian motion along the groove (see Video S2 in the supporting information). This result clearly demonstrates that QLLs existed in the grooves, even when we could not observe the macroscopic flow. Notably, in the case of the particles located on the grain surfaces, we observed no Brownian motion. Hence, we concluded that no macroscopically fluidic QLLs that could move the particles were present on the grain surfaces.

After similar observations, we also found that the temperature above which particles in grooves of grain boundaries started to move exhibited substantial variation (–1.9 ± 0.4 °C), as shown in Fig. 6A. This variation in temperature likely corresponds to the variation in the

characteristics of grain boundaries. This issue is an important topic that is left to future studies. Note that all polystyrene particles that we observed in the grooves of grain boundaries showed movement with increasing temperature. This result demonstrates that all particles were located not inside the grain boundaries but on the surfaces of the grooves; the particles were rejected by the growing ice–water interfaces[40] and then segregated on the groove surfaces during preparation of the sample. Hence, we observed particles located on the groove surfaces, although the focus depth of the LCM-DIM (7.5 μm)[19] was not sufficient to distinguish whether the particles were on the groove surfaces or inside the grain boundaries. However, we cannot exclude the possibility that the particles were partly trapped on the groove surfaces, which could also cause the substantial variation observed in Fig. 6A.

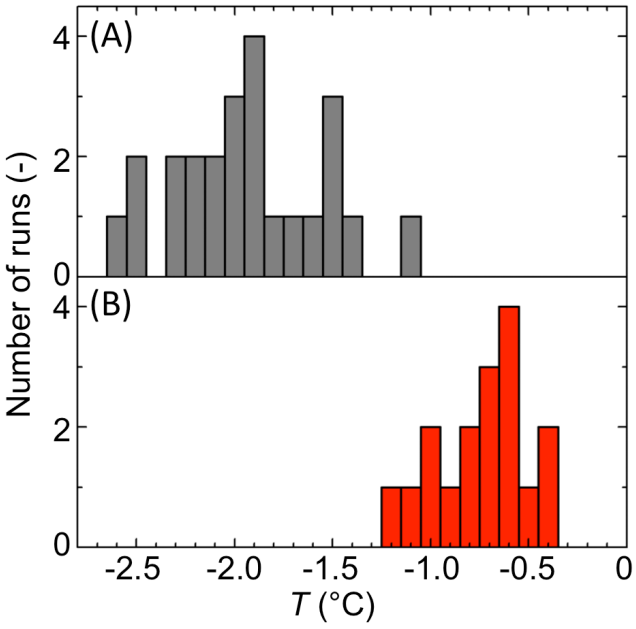

Fig. 6

Two experimental studies on the behavior of QLLs in grain boundaries in polycrystalline ice have been reported. Lu et al. concluded that the grain-boundary width was on the order of a few nanometers at −2 °C and that grain-boundary premelting was implausible at this temperature.[13] In addition, Thomson et al. also reported that the thickness of grain boundaries was in the range 1–10 nm for an undercooling of ~1.5 K.[15] However, Fig. 4 indicates that, to

observe the movements of particles in the grooves of grain boundaries, openings wider than the diameter of the particles (653 nm) needed to be filled with the QLLs. Hence, the possibility existed that the thickness of the grain boundaries was much larger than those reported by Lu et al.[13] and Thomson et al.[15] The optical microscope system used in the present study is a reflection-type microscope. Hence, we could not obtain any information related to the interior of the grain boundaries. To further study the interior of the grain boundaries, we are planning to develop a transmission-type optical system combined with the present setup.

3.3. QLLs on Grain Surfaces. We further increased the temperature and observed the ice grain surfaces again. A typical example is shown in Fig. 7, where we raised the temperature from –0.9 to –0.6 °C under various water vapor pressures. Figure 7A presents the time course of LCM-DIM images under supersaturated water vapor (P = 602 Pa and P_e = 582 Pa at point 7A in Fig. 3); P was on the border of the blue P–T region in which droplet-type QLLs exist kinetically and continuously on ice single crystals. After we raised the temperature from –0.9 to –0.6 °C, droplet-type QLLs appeared on the grain surface within a couple of minutes, as on the basal faces of ice single crystals.[33] In the present study, the differential interference contrast was adjusted as if the sample surface was illuminated by a light beam slanted from the lower-left to the upper-right direction. Hence, the lower-left and upper-right halves of the droplet-type QLLs appeared bright and dark, respectively. The white lines shown in the lower-left corners of the fields of view in Fig. 7 indicate a groove of a grain boundary between adjacent grains.

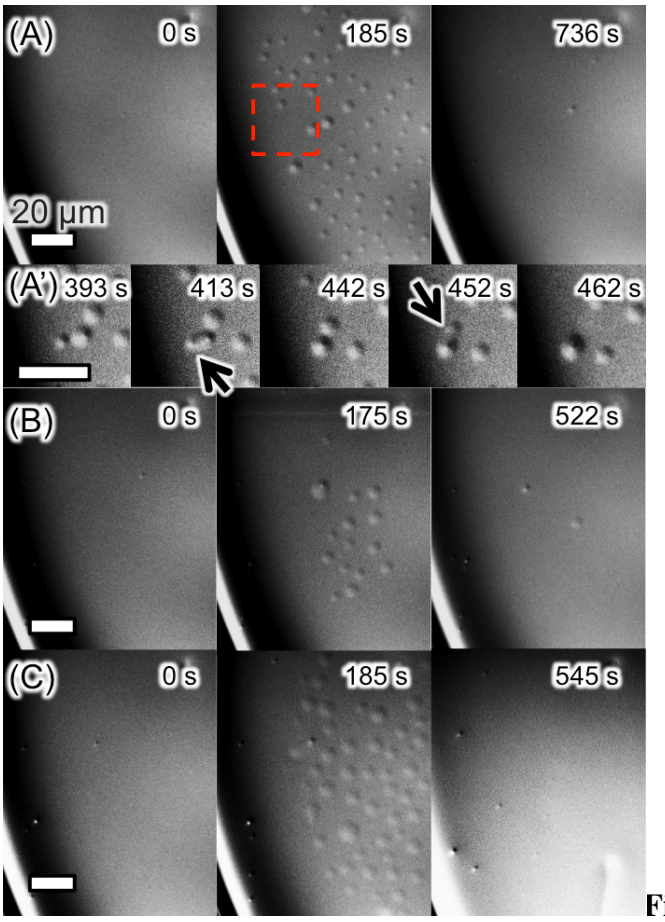

Fig. 7

Figure 7A′ shows the time course of LCM-DIM images in the area marked by the dotted rectangle in Fig. 7A (at 185 s). As time elapsed, adjacent droplet-type QLLs coalesced with each other at the positions marked by black arrows. This result clearly demonstrates that the droplet-type QLLs appearing on the grain surface exhibited macroscopic fluidity and that they were not a solid but a liquid formed on the grain surface at temperatures below 0 °C. Hence, they are appropriately referred to as QLLs.

In Fig. 7A, however, the droplet-type QLLs reached their maximum size (after 185 s) and then spontaneously disappeared (after 736 s) even though the temperature and water vapor pressure were kept constant. A video corresponding to Fig. 7A is available as Video S3 in the supporting information. Video S3 shows the spontaneous appearance and disappearance of the droplet-type QLLs and also their unidirectional motion from the upper-right to lower-left

direction. We did not observe such spontaneous disappearance of the droplet-type QLLs on surfaces of ice single crystals in the blue and red *P*–*T* regions in Fig. 3.

In addition, we performed similar observations to study the effects of water vapor pressure. Figures 7B and 7C also show the time course of LCM-DIM images taken in the immediate vicinity of the vapor–ice equilibrium curve (P = 578 Pa and P_e = 582 Pa, point 7B in Fig. 3) and under a highly undersaturated water vapor condition (P = 556 Pa and P_e = 582 Pa, point 7C in Fig. 3), respectively. As shown in Figs. 7B and 7C, even under these water vapor pressures, after we raised the temperature from –0.9 to –0.6 °C, drop-type QLLs appeared on the grain surface within a couple of minutes and then spontaneously disappeared within 10 min.

Using different samples, we performed similar observations under a wide range of water vapor pressures. Points 7X and 7Y in Fig. 3 show examples of such observations under a much higher water vapor pressure. Irrespective of the water vapor pressure, we confirmed the appearance and subsequent disappearance of droplet-type QLLs in a similar manner, although the temperature was slightly different. Figure 6B shows a summary of 17 runs. The temperature above which the droplet-type QLLs appeared on the grain surfaces but soon disappeared also substantially varied (–0.7 ± 0.2 °C). This variation in temperature is probably due to the variation in face indices of grain surfaces.

We previously reported that, on basal faces of ice single crystals, droplet-type and thin-layer-type QLLs exist kinetically in the blue and red *P*–*T* ranges in Fig. 3.[29, 30] In the present study, we apply the same concept, which is why, in the free energy diagram (Fig. 5), the QLLs on the grain surface (QLLs on G.S.) are thermodynamically more unstable (stable) than the ice crystal in supersaturated (undersaturated) conditions. Hence, in the pressure range marked by the double-headed green arrow in Fig. 3, the disappearance of the droplet-type QLLs on the grain surfaces does not conflict with the results obtained for basal faces of ice single crystals. Because

the droplet-type QLLs (a metastable phase) are more unstable than the ice crystal (the most stable phase), the ice grains grew, consuming the QLLs on the grain surfaces. However, on the grain surfaces of the polycrystalline ice thin film, as shown in Fig. 7, the droplet-type QLLs also disappeared even in the blue and red *P*–*T* ranges in Fig. 3 (demonstrated by points 7A–7Y). At present, the reason for this discrepancy is unclear. However, we propose two possible causes.

One possible cause is grain surfaces whose crystallographic orientations were random. Because such grain surfaces have a substantially higher kink density than basal faces of ice single crystals, the grain surfaces should grow via the adhesive-growth mechanism, which is usually substantially faster than the layer-by-layer growth.[41] Hence, the grain surfaces in contact with the droplet-type QLLs likely exhibited melt growth with markedly faster speed than the basal faces, resulting in the disappearance of the droplet-type QLLs on the grain surfaces. That is, the supersaturation and undersaturation of water vapor likely needed to be much higher to keep the droplet-type QLLs on the grain surfaces kinetically. To demonstrate this scenario, we attempted to observe the grain surfaces under much higher supersaturation. However, as the supersaturation was increased further, the number and size of the droplet-type QLLs on the grain surfaces increased and decreased dramatically, resulting in our inability to distinguish any events on the grain surfaces because of the limited spatial and temporal resolutions of our optical microscopy system.

The other possible cause is the appearance of the QLLs at $T \geq -1.9 \pm 0.4$ °C in the grooves of the grain boundaries (Figs. 4–6). Hence, at $T = -0.6$ °C, the droplet-type QLLs that formed on the grain surfaces coexisted with the QLLs located in the grooves of the grain boundaries. As shown in the free-energy diagram (Figs. 5A-2 and 5B-2), in a supersaturated (undersaturated) condition, the free energy of the QLLs on the grain surface (QLLs on G.S.) is higher (lower)

than that of the ice crystal because the QLLs on the grain surface are a metastable phase.[29,30] If the amount of QLLs in the grooves is much larger than the amount of droplet-type QLLs on the grain surfaces, the QLLs in the grooves can dominate the *P* distribution on the polycrystalline ice surface. Under a supersaturated (undersaturated) condition, the growth (evaporation) of the QLLs in the grooves can deplete (enrich) *P* in the vicinities of the grooves, and can eventually decrease (increase) *P* on the grain surfaces (see the free energy levels Vapor* (thick dotted lines) in Fig. 5), resulting in a decrease in the driving force for the growth of the droplet-type QLLs on the grain surfaces. To investigate this scenario, we need to further study the *P* distribution on the polycrystalline ice surfaces experimentally.

In addition to explaining the disappearance of the QLLs on the grain surfaces, we also need to explain their appearance, i.e., nucleation. As shown in Fig. 7B, we observed the appearance of droplet-type QLLs even in the vicinity of the vapor–ice equilibrium curve. This result implies that the nucleation of QLLs on the grain surfaces was enhanced compared with that on the basal faces. As already explained, the grain surfaces had a much higher kink density than the basal faces. Hence, such high-kink-density surfaces are reasonably assumed to be more liquid-like than basal faces and to thus have a smaller solid–liquid interfacial free energy. To investigate this scenario, we need to perform precise nucleation experiments in the future.

The disappearance of the droplet-type QLLs on the grain surfaces (Fig. 7) clearly demonstrates that our previous interpretation based on optical isotropy was incorrect,[18] as explained in our correction,[19] and that, after the disappearance of the droplet-type QLLs, the grain surfaces were dry even in the blue and red *P*–*T* ranges in Fig. 3. The results in the present study clearly demonstrate that grain boundaries play a primary role in the formation of QLLs on/in polycrystalline ice thin films.

One other issue warrants attention. On the surfaces of ice single crystals, 9-nm-thick thin-layer-type QLLs appear in addition to the droplet-type QLLs.[33, 34] However, on the grain surfaces of the polycrystalline ice thin films, the emergence of thin-layer-type QLLs was difficult to observe. Among all of the observations shown in Fig. 6, we observed thin-layer-type QLLs just three times and for limited durations, mainly because the grain surfaces of the polycrystalline ice thin films were substantially rougher than the basal and prism faces of ice single crystals. Figure 8 shows only one observation that enabled us to prepare relatively clear still images of thin-layer-type QLLs on the grain surfaces. In Fig. 8A1, a thin-layer-type QLL (red arrowhead) appeared on a grain surface and moved in the direction marked by the red arrow. As time elapsed, this QLL moved to the right side of the field of view and two thin-layer-type QLLs newly appeared at the left side (Fig. 8A2). The half-black/white arrowhead in Figs. 8A1 and 8A2 shows a hole formed just above a polystyrene particle buried inside the grain surface during growth; this hole can serve as a reference point. As shown in Fig. 8B, we also observed the coalescence of adjacent thin-layer-type QLLs at the point marked by the black arrow (this event is more easily observed in Video S4 in the supporting information). In the three observations, the temperatures at which the thin-layer-type QLLs appeared were –0.9, –0.9, and –0.3 °C (–0.7 ± 0.3 °C). Because of the experimental difficulty in visualizing the thin-layer-type QLLs on the grain surfaces, we lack experimental data concerning the disappearance and water-vapor-pressure dependence for the droplet-type QLLs.

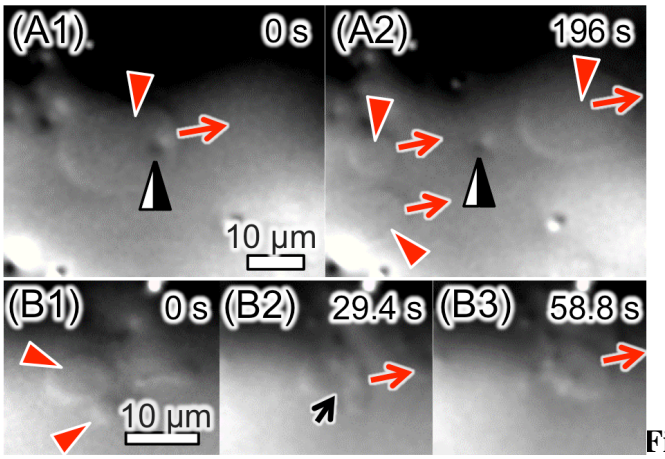

Fig. 8

4. CONCLUSIONS

In the present study, we observed polycrystalline ice thin films using the LCM-DIM. On the basis of the observed macroscopic fluidity, we determined the presence of QLLs. Our key results are summarized as follows.

1) With increasing temperature, the QLLs, which had sufficient volume to move the polystyrene particles, preferentially appeared in the grooves of grain boundaries at −1.9 ± 0.4 °C. The appearance of such QLLs was observed irrespective of the water vapor pressure (even at the vapor–ice equilibrium condition), indicating that these QLLs were formed by melting of the grain boundaries to eliminate the lattice mismatch between grains. After the QLLs appeared in the grooves, the QLLs continued to exist.

2) With increasing temperature, the droplet-type QLLs appeared kinetically on the grain surfaces at −0.7 ± 0.2 °C. However, they could not continuously exist on the grain surfaces and disappeared within 5 ± 3 min even though the temperature and water vapor pressure were kept constant. Hence, after the disappearance of the droplet-type QLLs, the grain surfaces were dry. These results suggest that the droplet-type QLLs on the grain surfaces were a metastable phase, like those on ice single-crystal surfaces.

3) With increasing temperature, thin-layer-type QLLs also appeared on the grain surfaces at temperatures higher than –0.7 ± 0.3 °C. However, because of the difficulty in visualizing these QLLs on rough grain surfaces, we have no data concerning their disappearance or water-vapor-pressure dependence.

Acknowledgements

The authors thank Y. Saito, S. Kobayashi, K. Ishihara, and G. Ryu (Olympus Corporation) for technical support with laser confocal microscopy, and Y. Furukawa (Hokkaido University) for valuable discussions. G.S. is grateful for partial support by JSPS KAKENHI (Grant No. 19H02611).

ASSOCIATED CONTENT

Supporting information: Captions of Videos S1–S4 in the supporting information. This material is available free of charge via the Internet at http://pubs.acs.org.

Web-Enhanced Feature:

Unidirectional movement of a polystyrene particle in a groove of a grain boundary at –2.3 °C (during the process of Fig. 4C) (Video S1), Brownian motion of a polystyrene particle in a groove of a grain boundary at –1.5 °C (P = 592 Pa and P_e = 540 Pa) (Video S2), appearance and subsequent disappearance of droplet-type QLLs on an ice grain surface at –0.6 °C (during the process in Fig. 7A) (Video S3), and coalescence of adjacent thin-layer type QLLs on an ice grain surface at –0.9 °C (during the process of Fig. 8B) (Video S4) are available as video files in the HTML version of the paper.

AUTHOR INFORMATION

Corresponding Author

Prof. Gen Sazaki: Institute of Low Temperature Science, Hokkaido University, N19-W8, Kita-ku, Sapporo 060-0819, Japan. E-mail: sazaki@lowtem.hokudai.ac.jp.

Phone and fax: +81-11-706-6880

Author Contributions

J.C., K.N., K.M., and G.S. designed the research performed by J.C. and G.S. T.M. produced a Linnik interferometer combined with a differential interference contrast microscope unit and also gave indispensable suggestions for optical observations. J.C. and G.S. wrote the paper. The authors declare no conflict of interest. All authors have given approval to the final version of the manuscript.

Funding Sources

JSPS KAKENHI (No. 19H02611).

ABBREVIATIONS

QLL: quasi-liquid layer, LCM-DIM: laser confocal microscopy combined with differential interference contrast microscopy

References

(1) Dash, J. G.; Rempel, A. W.; Wettlaufer, J. S., The physics of premelted ice and its geophysical consequences. *Rev. Mod. Phys.* **2006,** 78, 695-741.
(2) Wettlaufer, J. S.; Dash, J. G., Melting below zero. *Sci. Am.* **2000,** 282, 50-53.
(3) Petrenko, V. F.; Whitworth, R. W., *Physics of ice*. ed.; Oxford University Press: Oxford, 1999.
(4) Faraday, M., On certain conditions of freezing water. *Athenaeum* **1850,** 1181, 640.
(5) Dash, J. G., Thermomolecular pressure in surface melting - Motivation for frost heave. *Science* **1989,** 246, 1591-1593.
(6) Gilpin, R. R., Wire Regelation at Low-Temperatures. *J. Colloid Interface Sci.* **1980,** 77, 435-448.
(7) Sinha, P.; Muralidharan, S.; Sengupta, S.; Veerappapillai, S., A Brief Review on Antifreeze Proteins: Structure, Function and Applications. *Res. J. Pharm., Biol. Chem. Sci.* **2016,** 7, 914-919.
(8) Zhu, W.; Guo, J. M.; Agola, J. O.; Croissant, J. G.; Wang, Z. H.; Shang, J.; Coker, E.; Moteyalli, B.; Zimpel, A.; Wuttke, S.; Brinker, C. J., Metal-Organic Framework Nanoparticle-Assisted Cryopreservation of Red Blood Cells. *J. Am. Chem. Soc.* **2019,** 141, 7789-7796.
(9) Bartels-Rausch, T.; Jacobi, H.-W.; Kahan, T. F.; Thomas, J. L.; Thomson, E. S.; Abbatt, J. P. D.; Ammann, M.; Blackford, J. R.; Bluhm, H.; Boxe, C.; Domine, F.; Frey, M. M.; Gladich, I.; Guzmán, M. I.; Heger, D.; Huthwelker, T.; Klán, P.; Kuhs, W. F.; Kuo, M. H.; Maus, S.; Moussa, S. G.; McNeill, V. F.; Newberg, J. T.; Pettersson, J. B. C.; Roeselová, M.; Sodeau, J. R., A review of air–ice chemical and physical interactions (AICI): liquids, quasi-liquids, and solids in snow. *Atmos. Chem. Phys.* **2014,** 14, 1587-1633.
(10) Nagata, Y.; Hama, T.; Backus, E. H. G.; Mezger, M.; Bonn, D.; Bonn, M.; Sazaki, G., The Surface of Ice under Equilibrium and Nonequilibrium Conditions. *Acc. Chem. Res.* **2019,** 52, 1006-1015.
(11) Mader, H. M., Observation of the water-vein system in polycrystalline ice. *J. Glaciol.* **1992,** 38, 333-347.
(12) Mader, H. M., The thermal-behavior of the water-vein system in polycrystaline ice. *J. Glaciol.* **1992,** 38, 359-374.
(13) Lu, H.; McCartney, S. A.; Sadtchenko, V., Fast thermal desorption spectroscopy study of H/D isotopic exchange reaction in polycrystalline ice near its melting point. *J. Chem. Phys.* **2007,** 127, 184701-1-13.
(14) Thomson, E. S.; Wettlaufer, J. S.; Wilen, L. A., A direct optical method for the study of grain boundary melting. *Rev. Sci. Instrum.* **2009,** 80, 103903-1-7.
(15) Thomson, E. S.; Hansen-Goos, H.; Wettlaufer, J. S.; Wilen, L. A., Grain boundary melting in ice. *J. Chem. Phys.* **2013,** 138, 124707-1-5.
(16) Benatov, L.; Wettlaufer, J. S., Abrupt grain boundary melting in ice. *Phys. Rev. E* **2004,** 70, 061606-1-7.
(17) Thomson, E. S.; Benatov, L.; Wettlaufer, J. S., Abrupt grain boundary melting in ice (vol 70, 061606, 2004). *Phys. Rev. E* **2010,** 82, 039907-1.
(18) Chen, J. L.; Nagashima, K.; Murata, K.; Sazaki, G., Quasi-Liquid Layers Can Exist on Polycrystalline Ice Thin Films at a Temperature Significantly Lower than on Ice Single Crystals. *Cryst. Growth Des.* **2019,** 19, 116-124.
(19) Chen, J. L.; Maki, T.; Nagashima, K.; Murata, K.; Sazaki, G., Correction to "quasi-Liquid Layers Can Exist on Polycrystalline Ice Thin Films at a Temperature Significantly Lower than on Ice Single Crystals". *Cryst. Growth Des.* **2020,** 20, 4852-4854. DOI:10.1021/acs.cgd.8b01091

(20) Sazaki, G.; Matsui, T.; Tsukamoto, K.; Usami, N.; Ujihara, T.; Fujiwara, K.; Nakajima, K., In situ observation of elementary growth steps on the surface of protein crystals by laser confocal microscopy. *J. Cryst. Growth* **2004,** 262, 536-542.
(21) Sazaki, G.; Zepeda, S.; Nakatsubo, S.; Yokoyama, E.; Furukawa, Y., Elementary steps at the surface of ice crystals visualized by advanced optical microscopy. *Proc. Natl. Acad. Sci. U. S. A.* **2010,** 107, 19702-19707.
(22) Inomata, M.; Murata, K.-i.; Asakawa, H.; Nagashima, K.; Nakatsubo, S.; Furukawa, Y.; Sazaki, G., Temperature Dependence of the Growth Kinetics of Elementary Spiral Steps on Ice Basal Faces Grown from Water Vapor. *Cryst. Growth Des.* **2018,** 18, 786-793.
(23) Brandon, D. G.; Ralph, B.; Ranganathan, S.; Wald, M. S., Field ion microscope study of atomic conficuration at grain boundaries. *Acta Metall.* **1964,** 12, 813-821.
(24) Vold, C. L.; Glicksman, M. E., Behavior of grain boundaries near the melting point. In *The nature and behavior of grain boundaries: a symposium held at the TMS-AIME fall meeting in Detroit, Michigan*, Hu, H., Ed. Plenum Press: New York, 1971; pp 171-183.
(25) Watanabe, T., An approach to grain boundary design for strong and ductile polycrystals. *Res Mech.* **1984,** 11, 47-84.
(26) Higashi, A., Structure and behavior of grain boundaries in polycrystalline ice. *J. Glaciol.* **1978,** 21, 589-605.
(27) Hondoh, T.; Higashi, A., X-ray diffraction topographic observations of the large-angle grain boundary in ice under deformation. *J. Glaciol.* **1978,** 21, 629-638.
(28) Hondoh, T.; Higashi, A., Anisotropy of migration and faceting of large-angle grain-boundaries in ice bicrystals. *Philos. Mag. A* **1979,** 39, 137-149.
(29) Asakawa, H.; Sazaki, G.; Nagashima, K.; Nakatsubo, S.; Furukawa, Y., Two types of quasi-liquid layers on ice crystals are formed kinetically. *Proc. Natl. Acad. Sci. U. S. A.* **2016,** 113, 1749-1753.
(30) Murata, K.; Asakawa, H.; Nagashima, K.; Furukawa, Y.; Sazaki, G., Thermodynamic origin of surface melting on ice crystals. *Proc. Natl. Acad. Sci. U. S. A.* **2016,** 113, E6741-E6748.
(31) Asakawa, H.; Sazaki, G.; Nagashima, K.; Nakatsubo, S.; Furukawa, Y., Prism and Other High-Index Faces of Ice Crystals Exhibit Two Types of Quasi-Liquid Layers. *Cryst. Growth Des.* **2015,** 15, 3339-3344.
(32) Dehaoui, A.; Issenmann, B.; Caupin, F., Viscosity of deeply supercooled water and its coupling to molecular diffusion. *Proc. Natl. Acad. Sci. U. S. A.* **2015,** 112, 12020-12025.
(33) Sazaki, G.; Zepeda, S.; Nakatsubo, S.; Yokomine, M.; Furukawa, Y., Quasi-liquid layers on ice crystal surfaces are made up of two different phases. *Proc. Natl. Acad. Sci. U. S. A.* **2012,** 109, 1052-1055.
(34) Murata, K.; Asakawa, H.; Nagashima, K.; Furukawa, Y.; Sazaki, G., In situ Determination of Surface Tension-to-Shear Viscosity Ratio for Quasiliquid Layers on Ice Crystal Surfaces. *Phys. Rev. Lett.* **2015,** 115, 256103-1-5.
(35) Hilling, W. B., The kinetics of freezing of ice in the direction perpendicular to the basal plane. In *Growth and perfection of crystals*, Doremus, R. H.; Roberts, B. W.; Turnbull, D., Eds. Wiley: New York, 1958; pp 350-360.
(36) Pruppacher, H. R.; Klett, J. D., *Microphysics of clouds and precipitation*. ed.; Kluwer Academic Publishers: Dordrecht, 1997.
(37) Yokoyama, E.; Yoshizaki, I.; Shimaoka, T.; Sone, T.; Kiyota, T.; Furukawa, Y., Measurements of growth rates of an ice crystal from supercooled heavy water under microgravity conditions: basal face growth rate and tip velocity of a dendrite. *J. Phys. Chem. B* **2011,** 115, 8739-8745.
(38) Rozmanov, D.; Kusalik, P. G., Anisotropy in the crystal growth of hexagonal ice, I-h. *Journal of Chemical Physics* **2012,** 137, 094702-1-9.

(39) Wettlaufer, J. S.; Worster, M. G., Premelting dynamics. *Annu. Rev. Fluid Mech.* **2006,** 38, 427-452.
(40) Suzuki, Y.; Sazaki, G.; Hashimoto, K.; Fujiwara, T.; Furukawa, Y., Colloidal crystallization utilizing interfaces of unidirectionally growing ice crystals. *J. Cryst. Growth* **2013,** 383, 67-71.
(41) Chernov, A. A., Modern crystallography III. In *Springer Series in Solid-State Sciences*, Cardona, M.; Fulder, P.; Queisser, H.-J., Eds. Springerr-Verlag: Berlin, 1984; Vol. 36, pp 104-116.

Figure Captions

Fig. 1. Schematic of the custom-made observation chamber, a part of a laser confocal microscope combined with a differential interference contrast microscope (LCM-DIM), and a Linnik interferometer installed on the LCM-DIM. The observation chamber was made of upper and lower Cu plates whose temperatures T and T_{source} were separately controlled using Peltier elements. At the center of the upper Cu plate, a polycrystalline ice thin film prepared on a cover glass was attached using heat grease. Ice crystals for supplying water vapor to the polycrystalline ice thin film were grown on the lower Cu plate. A Nomarski prism for producing differential interference contrast could be easily substituted for the Linnik interferometer.

Fig. 2. A polycrystalline ice thin film and its grain growth behavior at $T = -2.1$ °C and $P = 534$ Pa ($P_e = 514$ Pa). (A) An LCM-DIM image of the polycrystalline ice thin film. (B) Time course of LCM-DIM images in the area marked by the dotted rectangle in image A. Image B1 corresponds to part of image A. The time indicated in images B2–B4 represent the elapsed time after image B1 was taken. Black arrows indicate grain boundaries exhibiting relatively fast grain growth and their direction of movement. (C) An LCM-DIM image showing all of image B4. Black arrowheads indicate grains that exhibit relatively slow grain growth.

Fig. 3. Pressure–temperature (*P*–*T*) phase diagram for water and the *P*–*T* regions in which QLLs exist kinetically and continuously on ice single crystals.[29, 30] On surfaces of ice single crystals, open squares (triangles) indicate critical water vapor pressures (temperatures) above which droplet-type QLLs exist kinetically; solid squares (triangles) indicate critical water vapor pressures (temperatures) above which thin-layer-type QLLs exist kinetically. Solid and dotted curves represent the vapor–ice and vapor–liquid water equilibrium curves, respectively. The rightmost and uppermost portions of the blue- and red-colored regions are shown by gradations in colors, indicating a lack of experimental datum; hence, the existence of QLLs is not indicated in these regions. Black and red arrows indicate the temperature changes (at constant pressures) induced in Figs. 4 and 7, respectively. Number–letter combinations beside the arrows correspond to figure numbers in Figs. 4 and 7. Red arrows 7X and 7Y are explained in the main text.

Fig. 4. The emergence of QLLs in a groove of a grain boundary of a polycrystalline ice thin film. (A) An LCM-DIM image of the polycrystalline ice thin film (T = –2.6 °C, P = 506 Pa and P_e = 492 Pa). White arrowheads show polystyrene particles (653 nm in diameter and 0.02% in volume fraction) located in the groove of the grain boundary and on the grain surface. (B to F) Time course of LCM-DIM images in the area marked by the dotted rectangle in image A: (B and B′) T = –2.6 °C, P = 602 Pa, and P_e = 492 Pa; (C) T = –2.3 °C, P = 602 Pa, and P_e = 505 Pa; (D) T = –2.3 °C, P = 506 Pa, and P_e = 505 Pa; (E) T = –2.3 °C, P = 501 Pa, and P_e = 505 Pa; and (F) T = –2.3 °C, P = 482 Pa, and P_e = 505 Pa. These *P*–*T* conditions correspond to points 4B–4F in Fig. 3. The temperature change from –2.6 to –2.3 °C (and also from –2.3 to –2.6 °C) occurred in less than 1 min. In images B–F, a time of 0 s corresponds to the moment at which the temperature became constant after the temperature change. In images B and B′, the polystyrene particles in the groove were fixed. By contrast, in images C, D, E and F, the

polystyrene particles moved along the groove as time elapsed. A movie of the process shown in C is available as Video S1.

Fig. 5. Free-energy diagrams for individual phases in (A) supersaturated and (B) undersaturated conditions, when QLLs (1) do not exist and (2) exist. The abbreviations G.B., G.G., and G.S. denote a grain boundary, a groove of a grain boundary, and a grain surface, respectively. (A-1) and (B-1) Because a grain boundary (a two-dimensional object) is not a phase, a dry grain boundary (Dry G.B.) here indicates a grain boundary and adjacent ice thin layers (slabs) in which the strain energy of the grain boundary is distributed. (A-2) and (B-2) With increasing temperature, the dry grain boundary is melted and QLLs are formed in the grain boundary. QLLs in G.B. show QLLs formed by the melting of the ice thin layers adjacent to the dry grain boundary. QLLs in G.G. present QLLs that appeared in a groove of a grain boundary. The QLLs formed on a grain surface (QLLs on G.S.) and the free energy level named Vapor* (thick dotted line) are discussed after Fig. 7.

Fig. 6. Two temperature ranges at which specific events occurred in grooves of grain boundaries (A: -1.9 ± 0.4 °C) and on grain surfaces (B: -0.7 ± 0.2 °C), respectively. (A) The variation of the temperature above which QLLs whose volume was sufficient to move the particles appeared in grooves of grain boundaries. (B) The variation of the temperature above which droplet-type QLLs appeared on grain surfaces but soon disappeared. The latter is discussed after Fig. 7.

Fig. 7. The emergence and subsequent disappearance of droplet-type QLLs on surfaces of ice grains at –0.6 °C (P_e = 582 Pa). Time course of LCM-DIM images of the grain surfaces were taken at (A) P = 602 Pa, (B) P = 578 Pa, and (C) P = 556 Pa. These P–T conditions correspond to points 7A–7C in Fig. 3. After the temperature was increased from –0.9 °C to –0.6 °C, the droplet-type QLLs appeared on the grain surface within a couple of minutes but subsequently

disappeared gradually from the grain surface as additional time elapsed. The temperature increase from –0.9 to –0.6 °C occurred in less than 1 min. In images A–C, a time of 0 s corresponds to the moment at which the temperature started to increase. Images A′ also show a detailed time course of enlarged LCM-DIM images in the area marked by the dotted rectangle in image A (at 185 s) during process A. Adjacent droplet-type QLLs coalesced with each other at the positions marked by black arrows, clearly demonstrating macroscopic fluidity of the droplet-type QLLs. All scale bars correspond to 20 μm. A movie of the process shown in A is available as Video S3.

Fig. 8. The emergence of thin-layer-type QLLs on grain surfaces at T = –0.9 °C and P = 593 Pa (P_e = 568 Pa). (A) A thin-layer-type QLL (red arrowhead) appeared on a grain surface (image A1) and moved in the red-arrow direction. In image A2, the thin-layer-type QLL shown in image A1 moved to the right side of the field of view and two thin-layer-type QLLs newly appeared in the left side. The half-black/white arrowhead represents a hole formed just above a polystyrene particle buried inside the grain surface during growth. (B) Two adjacent thin-layer-type QLLs (read arrowheads) coalesced with each other at the point marked by the black arrow. In these images, a time of 0 s only indicates the moments at which images A1 and B1 were taken and therefore does not correspond to the duration after the temperature change. Because all panels show magnified images, no grain boundary is shown. A movie of the process shown in B is available as Video S4, where the movement event is easily observed.

For Table of Contents Use Only

Quasi-liquid layers in grooves of grain boundaries and on grain surfaces of polycrystalline ice thin films

Jialu Chen, Takao Maki, Ken Nagashima, Ken-ichiro Murata, Gen Sazaki

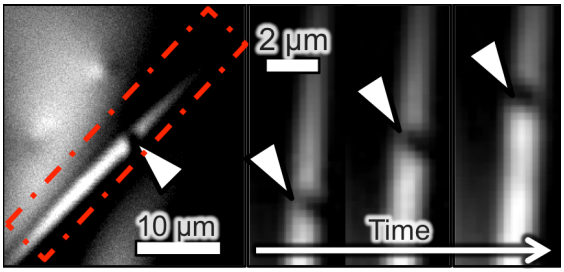

Synopsis (60 words ≤ 60 words)

We observed surfaces of polycrystalline ice thin films using our advanced optical microscope and found that, with increasing temperature, QLLs first appeared preferentially in grooves of grain boundaries at –1.9±0.4 °C. With an increasing temperature, droplet-type QLLs appeared on grain surfaces at –0.7±0.2 °C but spontaneously disappeared within 5±3 min even though the temperature and water vapor pressure were constant.